Electrochemistry Communications 147 (2023) 107435

Contents lists available at ScienceDirect

Electrochemistry Communications

journal homepage: www.elsevier.com/locate/elecom

Understanding the behaviour of a niobium oxide cathode in a molten chloride bath using different DC voltammetric techniques

Heba Mashaal [a], Ahmed Abdelkarim [a], Ahmed Dawood [a], Hussein Abd El-Aziz [b], Hany Gamal [a], Abd Allh M. Abd El-Hamid [a], Hamed Mira [a], Amr M. Abdelkader [c,*]

[a] Nuclear Materials Authority, PO Box 530, El Maadi, Cairo, Egypt
[b] Faculty of Engineering, Al-Azhar University, Cairo 11371, Egypt
[c] Faculty of Science and Technology, Bournemouth University, Talbot Campus, Fern Barrow, Poole BH12 5BB, UK

ARTICLE INFO

Keywords:
FFC-Cambridge process
Molten salt
High-temperature electrochemistry
Electrorefining
High-temperature materials

ABSTRACT

The electro-deoxidation of metal oxides has been presented as an alternative to the pyro- and electro-metallurgical techniques generally used to create metals and alloys. However, previous research has concentrated on employing chronoamperometric techniques to analyse cathodic reactions, ignoring important information on reduction processes. In this work, we examine electro-deoxidation using several DC voltammetric techniques, including constant potential chronoamperometry, sampled-current voltammetry, linear sweep voltammetry, and constant current chronopotentiometry. Niobium pentoxide was taken as the model cathode material. As a result, the following reduction mechanism is proposed: (1) Nb (V) oxidation state, represented by the compounds Nb_2O_5, $CaNbO_6$, and $Ca_2Nb_2O_7$, reduced to Nb (IV) in the compounds NbO_2 and $CaNbO_3$; (2) Nb (IV) reduced to Nb (III) in the form of $CaNb_2O_4$; (3) $CaNb_2O_4$ reduced quickly to NbO, which is the only form of Nb(II); the latter is reduced to Nb(0) by the end of the electro-deoxidation process. The results show that NbO partially dissolves in the electrolyte and suggest the creation of two distinct soluble niobium complexes, depending on the oxygen level of the electrolyte.

1. Introduction

Fray and his co-workers have developed an electrometallurgical process as an alternative to the traditional industrial processes for producing metals and alloys. In this process, a metal oxide cathode is electro-deoxidised to the corresponding metal by applying enough potential to ionise the cathode's oxygen. The oxide ions then migrate through the molten salt electrolyte towards a graphite anode, where they are discharged in the form of carbon oxide gases [1]. A significant number of laboratory studies have since concentrated on the electrolytic production of numerous metals such as Ti, Th, Gr, Si, Nb, Cr, Hf, Zr; binary alloys and intermetallics such as Co-Cr, W-Ti, $NdCo_5$; ternary alloys such as Nb–Hf–Ti, Ti–6Al–4V; and quaternary alloys such as Ti–29Nb–13Ta–4.6Zr and CoCrFeNi [2–6]. The method has also been used to create nano and micro-sized particles of mono and binary carbides and oxycarbides [7–11]. Furthermore, it has been utilised to synthesise graphene by electrochemically reducing graphene oxide and to recover oxygen from lunar regolith [12,13]. The benefits of the FFC-Cambridge process over other extractive metallurgy processes are its simplicity, relatively low energy needs, relatively low labour requirements, and the ability to directly reduce a mixture of various metal oxides to produce alloys.

During the operation of the FFC-Cambridge process, many different voltammetric techniques have been used to understand the reduction mechanism or to optimise the process parameters. These include constant voltage, constant potential, cyclic voltammetry and constant current methods [14]. However, no reported work has applied these techniques together to build a good understanding of the electro-deoxidation process for a specific oxide. Using Nb_2O_5 as a case study, the current work demonstrates that a significant amount of information can be gathered by using different DC voltammetric techniques, improving our understanding of the mechanism and kinetics of the electro-deoxidation process and aiding in the development of a portfolio of electro-deoxidation reactions.

* Corresponding author.
E-mail address: aabdelkader@bournemouth.ac.uk (A.M. Abdelkader).

https://doi.org/10.1016/j.elecom.2023.107435
Received 2 December 2022; Received in revised form 5 January 2023; Accepted 8 January 2023
Available online 9 January 2023

2. Experimental

Details of the experimental setup and the characterization of the starting material are given in the Supplementary Information.

3. Results and discussion

3.1. Constant potential chronoamperometry

The electro-deoxidation of the niobium pentoxide cathode was first studied under constant potential to ensure process control and clarify the cathodic reactions [14]. To minimise calcium metal deposition, the potential window for $CaCl_2$–1 mol.% CaO was established using a graphite working electrode and a graphite pseudo reference electrode. The cathodic part of the voltammogram is presented in Fig. S2 (see Supporting Information). The calcium deposition potential can be calculated from Fig. S2 as –1.29 V versus the graphite pseudo reference, using the tangency method [15]. This value is consistent with previous studies of the same system [16,17].

To reduce calcium deposition, the cathode's applied potential was set to less than −1.29 V. The current response during 10 h of electro-deoxidation at constant potentials of −1.25 V, −1.15 V, −1.05 V, −0.950 V, and −0.85 V vs a graphite pseudo reference is shown in Fig. 1. The time–current charts indicate the same pattern for the specified potential range: when the cathodic potential is applied, the current quickly increases and then steadily drops in the first few hours before approaching a time-independent value for the duration of the run. It can also be seen from Fig. S3 that the initial current and the value of the time-independent current in the final stage of electro-deoxidation increase as the potential becomes more negative. Increases in the background current may be due to the calcium activity created in the melt. The total charge passed increases with the cathodic potential, up to –1 V, and then remains almost constant (as determined by the area under the curve).

According to the XRD pattern, the two samples electro-deoxidised at −0.85 V and −0.95 V were mostly composed of calcium niobate and NbO_2 (Fig. 2). Only Nb can be identified in the XRD and EDX spectra at potentials greater than −1.05 V. These results might explain the behaviour of the current–time plot that shows the same charge passed during the electro-deoxidation of Nb_2O_5 at potentials more negative than –1 V. As the amount of Nb_2O_5 is the same in each run, the charge required for complete reduction should be the same. Therefore, increasing the potential leads to an increase in the rate of electro-deoxidation, as indicated by the current approaching the background value faster at more negative cathodic potentials.

For potentials more cathodic than –1.05 V, samples were taken at the start of the steady-state current step to determine the nature of this stage. Although the XRD analysis detects only metallic niobium, the measured oxygen content ranged between 2.4 and 1.8 wt%, as shown in Table S1. These values are higher than the solubility limit of oxygen in solid niobium at room temperature [18]. The high oxygen content of the sample and the absence of any oxide phase in the XRD pattern are consistent with the fact that NbO particles were not detected by X-ray diffraction. As is apparent from the SEM of the produced powder (Fig. 3), niobium particles tend to sinter together in the form of agglomerates. Some niobium oxides could also be trapped in the intergranular boundaries in small fractions below the detection limit of XRD. However, the SEM analysis (Fig. 4) detected some well-defined cubic grains with sharp edges (Fig. 4). The EDX showed the chemical composition of these cubes to be 52 atomic % niobium and 48 atomic % oxygen, which proves the presence of NbO.

3.2. Sampled-current voltammetry

From an energy standpoint, it is preferable to use the lowest feasible potential on the cathode. Sampled-current voltammetry is suitable for determining this critical potential (SCV). Normal pulse voltammetry (NPV) is the simplest type of SCV and the most relevant to the electro-deoxidation process. In classic NPV, a series of potential pulses with increasing amplitude are imposed on the working electrode. The resulting current response is similar to that obtained from the electro-deoxidation process, i.e. a decline over time to a steady state value. The difference is that in NPV, the current is capacitive in nature (from the charging of the double layer), while the current in the electro-deoxidation process is Faradaic. Hence, in classical NPV, the current is measured near the end of each pulse to exclude double-layer charging.

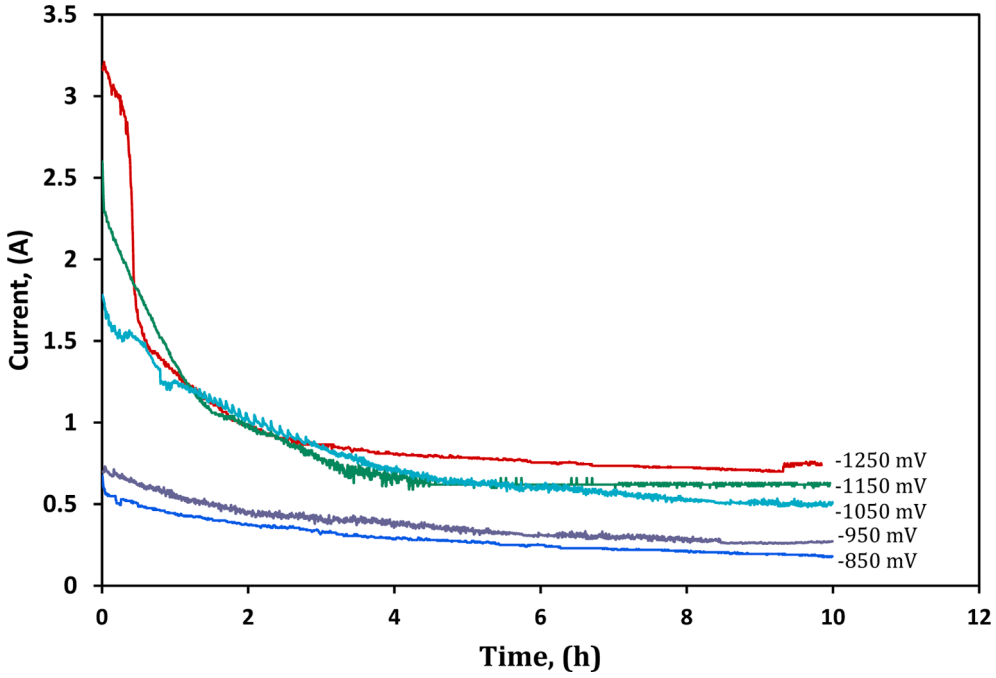

Fig. 1. Typical *I–t* plots recorded during potentiostatic electrolysis of a Nb_2O_5 pellet in molten CaO-$CaCl_2$ (1173 K) at the indicated potentials (versus a graphite pseudo reference).

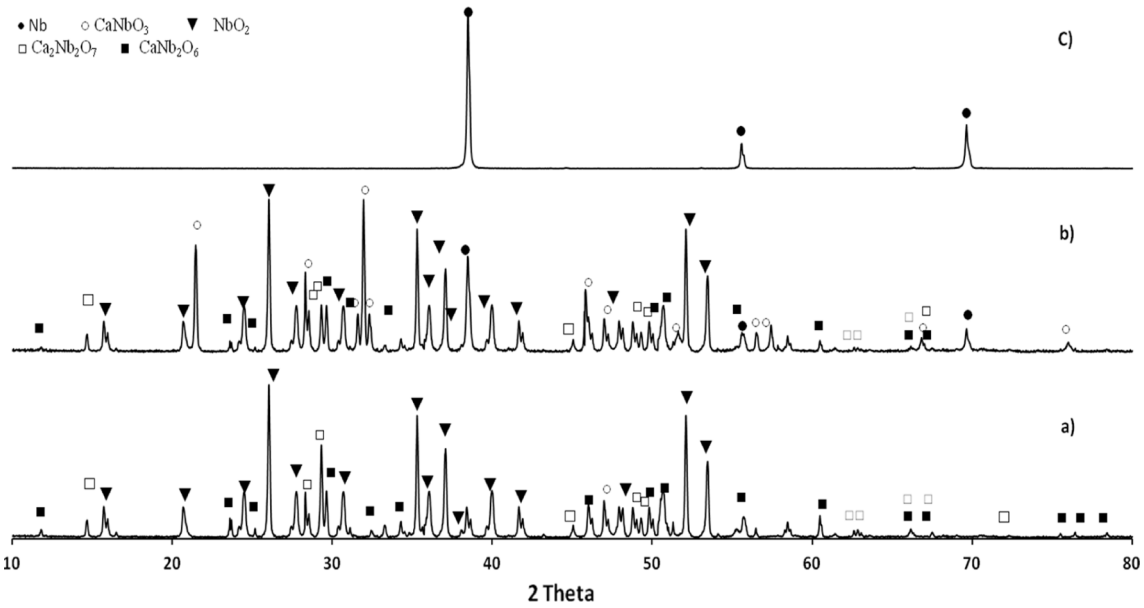

Fig. 2. XRD patterns of a Nb_2O_5 pellet electro-deoxidised for 10 h in molten CaO-$CaCl_2$ at three different constant potentials: (a) –0.85 V, (b) –0.95 V, and (c) –1.15 V.

The current is then plotted versus the potential at which the step takes place. In the electro-deoxidation process, the concentration of the ionised species on the cathode (the oxygen ions) approaches a negligible value as the current approaches the steady state. Therefore, a sampled-current voltammogram could be assembled if we consider every curve in the time–current plot represented in Fig. 1 as a response for a single plus step.

However, the current represented in Fig. 1 involves a non-negligible portion of residual current due to the electronic conductivity of the molten salt [19]. This residual current must be subtracted from the total value to calculate the effective fraction of the current due to electro-deoxidation. Therefore, a series of experiments were conducted to record the residual current on the empty cup cathodes at different potentials. Figure S3 shows the average value of the current measured on a blank stainless steel cup at different potentials and the variation of the effective current as calculated from Fig. 1.

The sampled-current voltammogram is constructed by sampling the current at some fixed time (τ) in each potential step. Fig. 5 represents the $i(\tau)$–E curve with τ chosen to be 7 h. The current–potential curve has a wave shape similar to that obtained from classical NPV. The ionisation of oxygen from the Nb-O solid solution is responsible for this limiting value. This limiting current is the distinguishing feature of the mass-transfer-limited region, analogous to the sampled-current voltammogram in aqueous solutions. Due to oxygen depletion at the cathode, the surface concentration approached zero, and the electrochemical reactions occurred as fast as diffusion brought the oxygen atoms to the surface where ionisation occurred. This factor limits the current, and the potential no longer influences the electrolytic current. It should be mentioned here that three-phase interline (3PI) models are not applicable due to the metallic nature of the cathode. Therefore, a potential of –1.1 V vs a graphite pseudo reference is optimum to reduce Nb_2O_5 in a three-terminal electro-deoxidation experiment conducted under constant potential chronoamperometry.

The story is different for potentials lower than –1 V. The XRD, SEM, and EDX analyses reveal a non-metallic powder, with calcium niobate and niobium dioxide as the main constituents. In this case, oxygen diffuses to the metal/metal oxide/electrolyte 3PIs only through the partial reduction of the niobium pentoxide according to reactions (1)–(3). The amount of oxygen and the rate of delivery to the electrode surface (the 3PI) are significantly lower than in circumstances when complete reduction occurs. The Faradaic current approaches zero once the conversion of Nb(V) (Nb_2O_5, $CaNb_2O_6$, and Ca_2NbO_7) to Nb(IV) (NbO_2, $CaNbO_3$) is complete. Furthermore, Nb(II) dissolution in the melt at lower applied potentials (as detailed in the Supporting Information) and its interaction with other electroactive species in the electrolyte consume a portion of the non-Faradaic current.

$$Nb_2O_5 + CaO = CaNb_2O_6\ \Delta G^o = \text{-}148.286\ \text{kJ (at 1173 K)} \quad (1)$$

$$2Nb_2O_5 + Ca^{2+} + 2e^- = CaNb_2O_6 + 2NbO_2\ E^o = 2.27\ \text{V}\ (Ca^{2+}/Ca)\ \text{(at 1173 K)} \quad (2)$$

$$3Nb_2O_5 + 2Ca^{2+} + 4e^- = Ca_2Nb_2O_7 + 4NbO_2\ E^o = 2.27\ \text{V}\ (Ca^{2+}/Ca)\ \text{(at 1173 K)} \quad (3)$$

3.3. Constant current chronopotentiometry

The results of linear sweep voltammetry (see Supporting Information) showed that the oxide pellet lost mass during the electro-deoxidation of Nb_2O_5 owing to the dissolving of the intermediate phase, NbO, in the molten salt. Depending on the applied voltage, this mass loss was observed to be either partial or complete. As a result, it is preferable to investigate electro-deoxidation using a more sensitive potential approach. Constant current chronopotentiometry measures the electric potential response of a system to an imposed current. It maintains the working electrode's potential at a value characteristic of the redox couple and changes with time. When the concentration of ions in the vicinity of the working electrode approaches zero, the potential shifts to a more negative value, where a second Faradaic process can support the current. Compared to other dynamic characterisation methods, such as impedance spectroscopy, and cyclic amperometry or voltammetry, this approach allows correlation of significant transient states with the measured electric potential. Differences in electric potentials indicate differences in transport conditions.

A typical chronopotentiogram of Nb_2O_5 electro-deoxidation using a constant current of 0.5 A across a two-terminal cell is illustrated in Fig. 6. The cathodic potential measured versus a graphite pseudo reference shows three notable features before calcium deposition: a plateau value of about –0.5 V for the first two hours, followed by a gradual increase in the potential for another 1.5 h, and another plateau

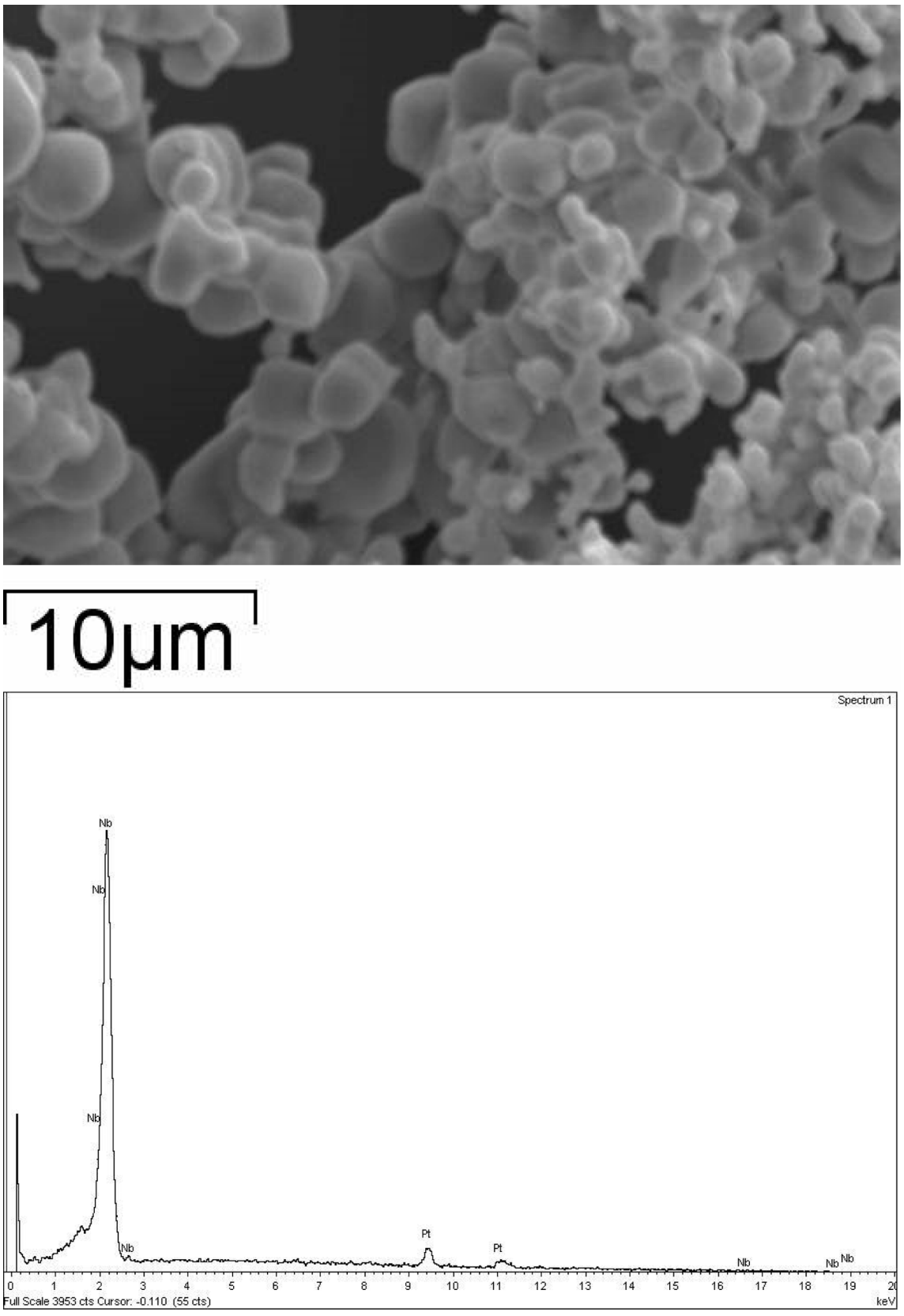

Fig. 3. SEM image and EDX spectra of the niobium powder obtained from the electro-deoxidation of a Nb_2O_5 pellet at a constant potential of –1.15 V (versus a graphite pseudo reference).

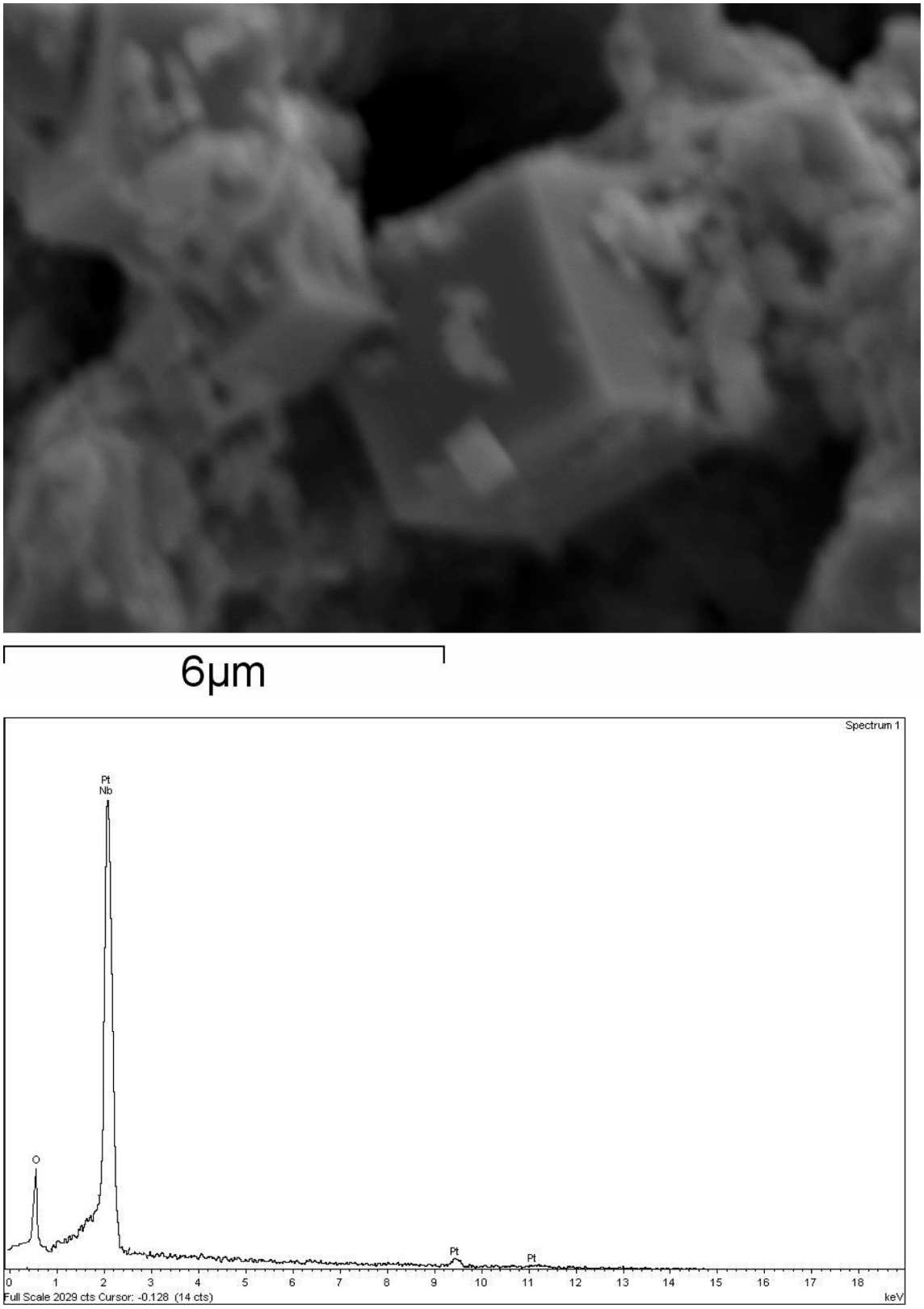

Fig. 4. SEM image of a cubic crystal trapped between metallic niobium particles. The EDX spectrum detects 48 atomic% oxygen.

at about –1.1 V. The potentials of the two plateaux have almost the same values as the two peaks observed in the LSV voltammogram if one considers the higher iR drop of the constant current experiments. This potential behaviour confirms that the electro-deoxidation of niobium pentoxide takes place in three major steps.

The first plateau depicts the reduction of Nb(V) to Nb(II) and Nb(0) via reactions (4–9.7), which occur at around −0.5 V. The progressive increase in cathodic potential after the first two hours is due to the reduction of $CaNbO_3$ to NbO (reaction (S2) in SI). The third plateau represents the reduction of Nb(II) (in the form of NbO) to Nb(0)

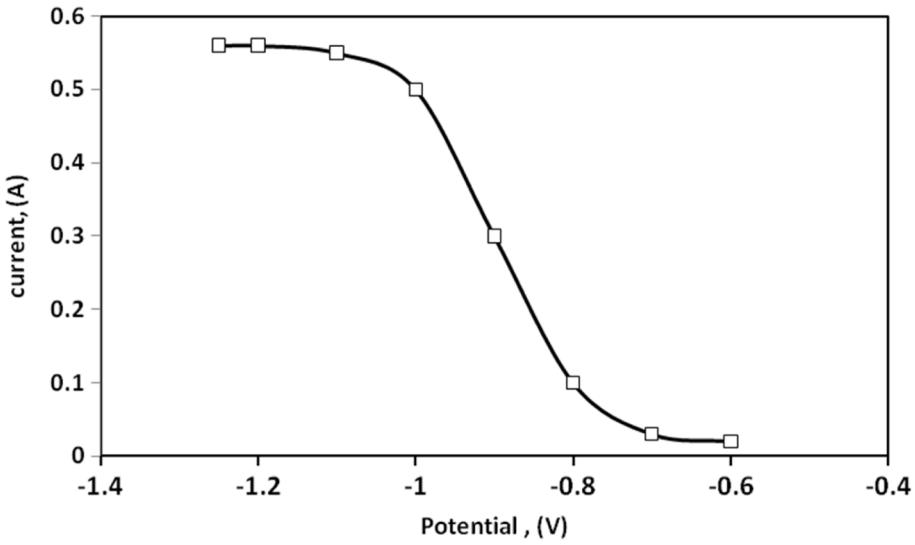

Fig. 5. Sampled-current voltammogram for the electro-deoxidation of a Nb_2O_5 pellet in molten CaO-$CaCl_2$, in which the current was measured after 7 h and the potentials were measured versus a graphite pseudo reference.

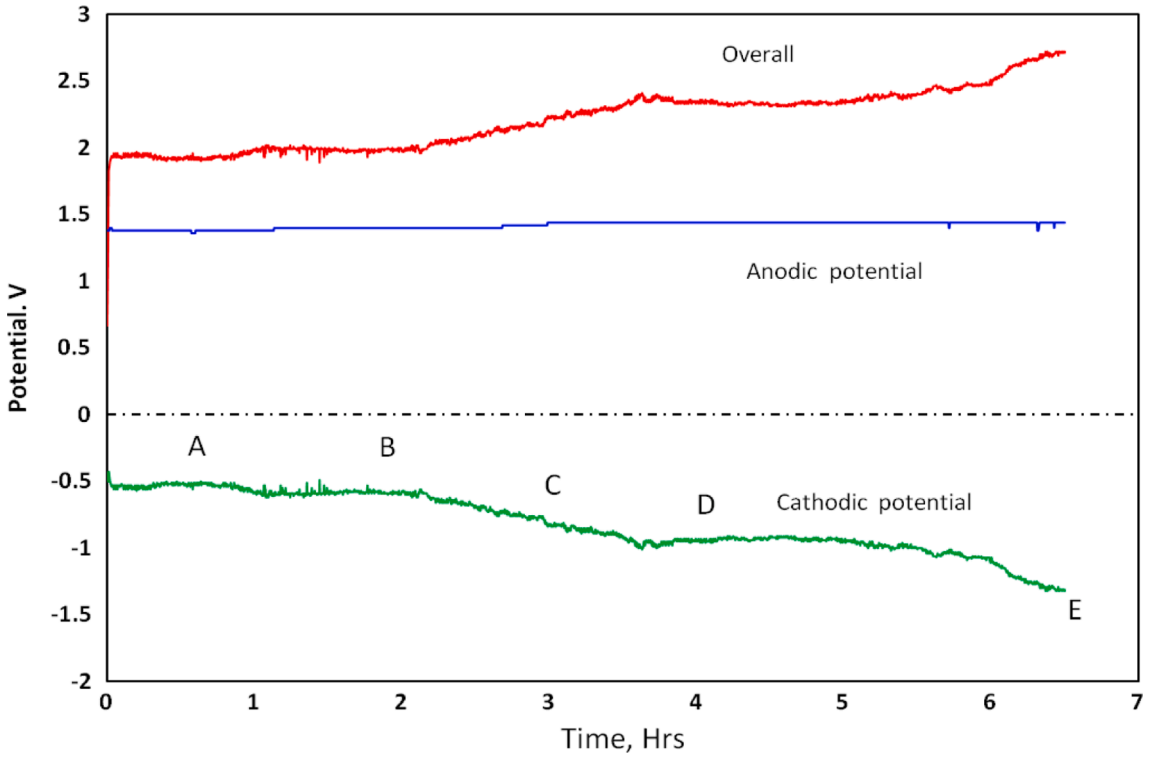

Fig. 6. Chronopotentiogram for the electro-deoxidation of Nb_2O_5 in molten CaO-$CaCl_2$ recorded at 0.5 A.

(metallic niobium) according to reaction (8). The mechanisms listed in equations (4)–(8) and equations S2–S3 in the SI were verified by interrupting the reduction after 0.5, 1.5, 2.5 and 4 h, labelled as A–D in Fig. 6. The product was analysed using XRD, and the results are shown in Fig. 7. It is worth mentioning here that the XRD detected no NbO in any partially reduced sample.

$$2NbO_2 + Ca^{2+} + 2\,e^- = CaNbO_3 + NbO \quad (4)$$

$$CaNb_2O_6 + 4\,e^- = CaNbO_3 + NbO + 2O^{-2} \quad (5)$$

$$2NbO_2 + Ca^{2+} + 4e^- = CaNbO_3 + Nb + O^{-2} \quad (6)$$

$$CaNb_2O_6 + 6\,e^- = CaNbO_3 + Nb + 3O^{-2} \quad (7)$$

$$NbO + 2\,e^- = Nb + O^{2-}9 \quad (8)$$

About 25% of the niobium content was missing from the fully reduced sample. To clarify that the dissolution of NbO caused the loss of niobium from the cathode materials, samples from the electrolyte were taken in situ during the electro-deoxidation at fixed intervals of 0.5 h. The first detection of niobium ions was in the sample collected after 1.5 h from the start of electro-deoxidation, i.e. during the stage in which NbO is produced by reactions 9 and 10. Furthermore, the Nb:Ca mol. ratio was about 1.05 in the partially reduced pellet electro-deoxidised up to point C, as measured by EDX (Fig. 8). Based on XRD analysis of the

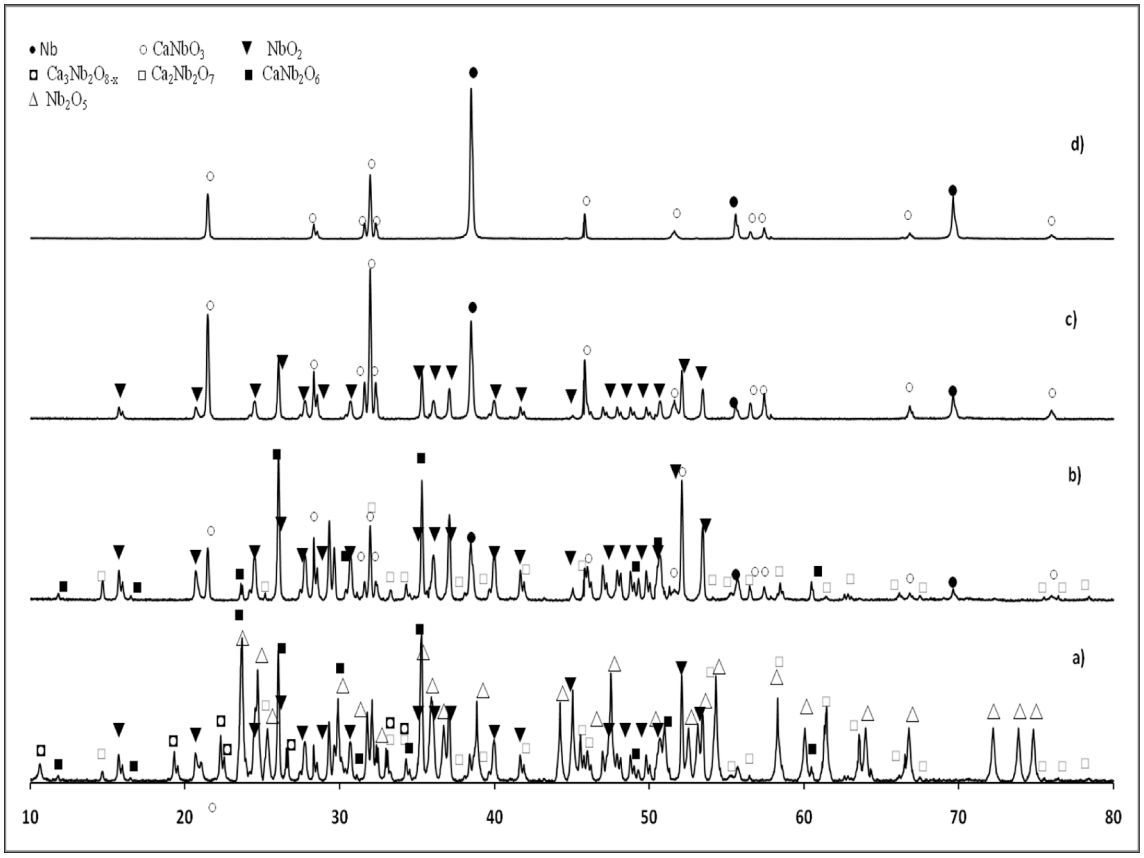

Fig. 7. XRD pattern for the Nb_2O_5 pellet electro-deoxidised at 0.5 A constant current in molten CaO-$CaCl_2$ after (a) 0.5 (b) 1.5 (c) 2.5, and (d) 4 h.

same sample, this value must be higher than 1.05, as metallic niobium was detected in a reasonable quantity, indicating that some niobium had gone missing from the cathode material at this point.

When a constant current of 0.2 A was applied, the potential–time curve was different to that recorded at 0.5 A. The cathodic potential recorded at a low applied current (Fig. 9) shows a plateau value in the first 2 h, corresponding to the transformation of Nb_2O_5 in the core of the pellet to $CaNb_2O_6$ and $Ca_2Nb_2O_7$, with the emergence of NbO_2 as a byproduct of the reaction. Terminating the experiments after 1 h and analysing the sample proved the coexistence of all the Nb(IV) phases with some NbO_2. Once the formation of the high calcium content niobate had finished, the potential behaviour was more or less similar to that recorded at a constant current of 0.5 A; and is as follows: (1) A plateau between 2 and 9 h at around –0.5 V corresponding to the reduction of Nb(V) to Nb(IV), as revealed from the XRD trace for the sample taken after 3 h; (2) A gradual increase in the potential up to a value of –1.1 V which, by analogy with the reduction at a constant current 0.5 A, can be attributed to the reduction of Nb(V) to Nb(II); and (3) A short pseudo steady state at a potential value of –1.1 V corresponding to the reduction of Nb(II) to Nb(0) (again analogous with curve 4–19). (4) Finally, the potential shifted to the value at which calcium metal is deposited from the electrolyte (-1.3 V).

During feature (2), the pellet completely dissolved in the electrolyte. Under 0.2 A constant current chronopotentiometry, the reduction of NbO to Nb is slow, allowing NbO to dissolve in the electrolyte. The pellet holder removed after 11 h of electro-deoxidation showed traces of $CaNbO_3$ powder. However, no niobium deposit was observed on the holder or on the current collector. It was only after 12 h, corresponding to feature (4), that the first niobium deposit was observed on the holder. As the potential value of the last plateau was almost the same whether a constant current of 0.2 A or 0.5 A was applied, this plateau must correlate to the same number of electrons transferred in both cases, i.e. corresponding to the reduction of the same oxidation state, which is evidence that niobium was dissolved and redeposited in the (II) oxidation state. If niobium ions were oxidised on the anode and dissolved in the electrolyte, another plateau would be observed before feature (4).

4. Conclusion

In this paper, the electro-deoxidation of the niobium pentoxide cathode in a molten chloride bath has been investigated. The cathodic processes were studied using various DC techniques, including constant potential, sampled current voltammetry, linear sweep voltammetry, and constant current chronopotentiometry. The results suggested that the reduction starts by forming calcium niobate in the form $CaNb_2O_6$ and $Ca_2Nb_2O_7$ (in which niobium is Nb(V)). The Nb(V) niobate was then reduced to Nb(IV) and then to Nb(II) through a very rapid reduction step of Nb(III) and then to metallic niobium. The results obtained from the constant potential experiments demonstrated mass loss of the oxide pellet during the electro-deoxidation of Nb_2O_5 due to the dissolution of the intermediate phase, NbO, in the molten salt. Depending on the applied potential, this mass loss was reported to be partial or full. This dissolution was further studied by constant current chronopotentiometry. The CP allowed the potential to stabilise at certain values associated with electrochemical steps. The chronopotentiogram recorded at a constant current of 0.2 A showed a plateau at the value where NbO reduces to Nb. The pellet completely dissolved at this point, and Nb was redeposited afterwards on the metallic holder. The sample electro-deoxidised at 0.5 A constant current showed only partial dissolution, suggesting that this depends on kinetic conditions.

CRediT authorship contribution statement

Heba Mashaal: Writing – original draft, Methodology, Data

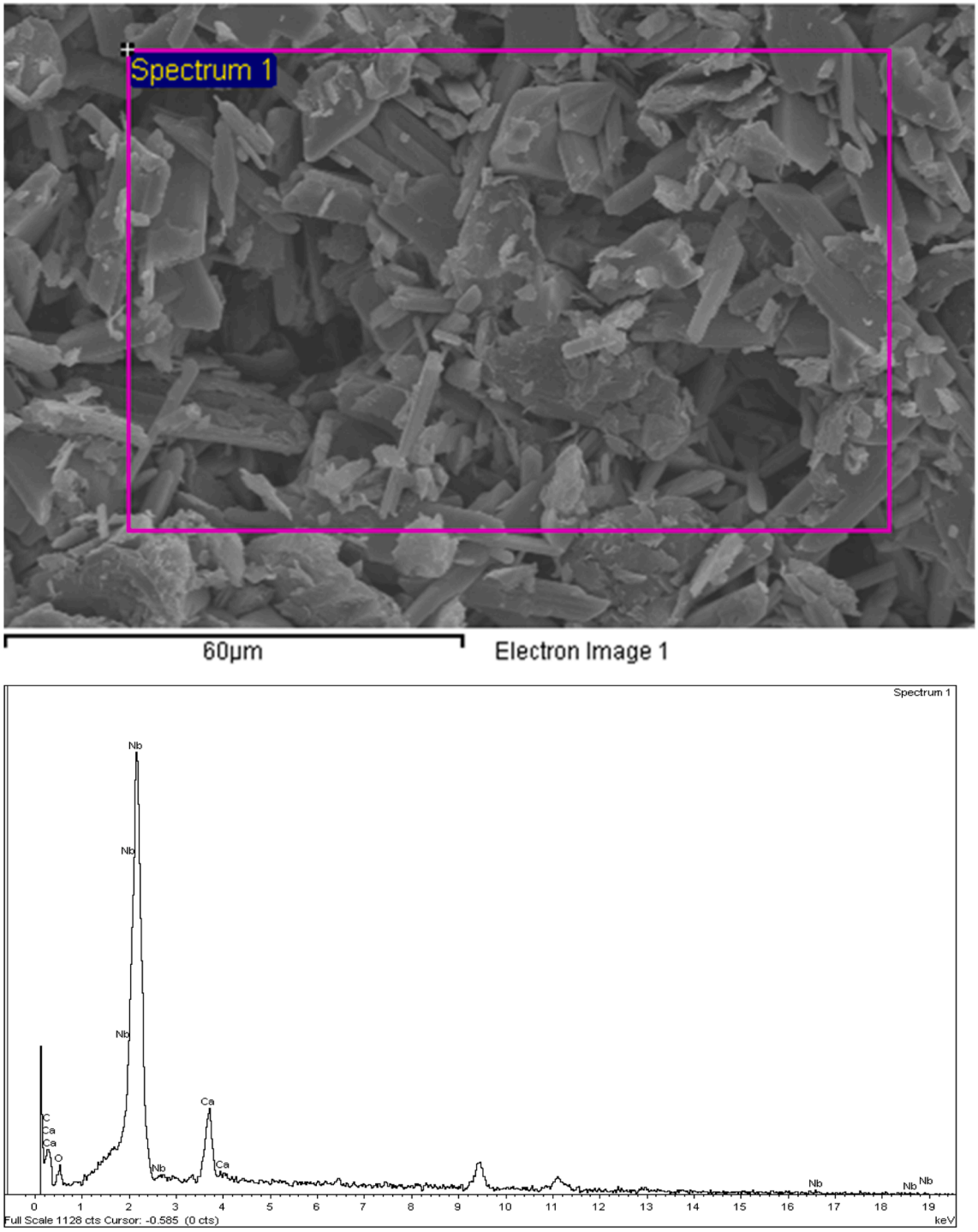

Fig. 8. SEM image and EDX spectrum for the powder obtained after 3 h of Nb_2O_5 pellet electro-deoxidation at a constant current of 0.5 A.

curation, Visualization, Investigation, Writing – review & editing. **Ahmed Abdelkarim:** Writing – review & editing, Visualization, Supervision. **Ahmed Dawood:** Investigation, Methodology, Writing – review & editing. **Hussein Abd El-Aziz:** Data curation, Methodology. **Hany Gamal:** Investigation, Supervision. **Abd Allh M. Abd El-Hamid:** Writing – review & editing. **Hamed Mira:** Visualization, Supervision. **Amr M. Abdelkader:** Conceptualization, Supervision, Writing – review & editing.

Declaration of Competing Interest

The authors declare that they have no known competing financial interests or personal relationships that could have appeared to influence the work reported in this paper.

Data availability

Data will be made available on request.

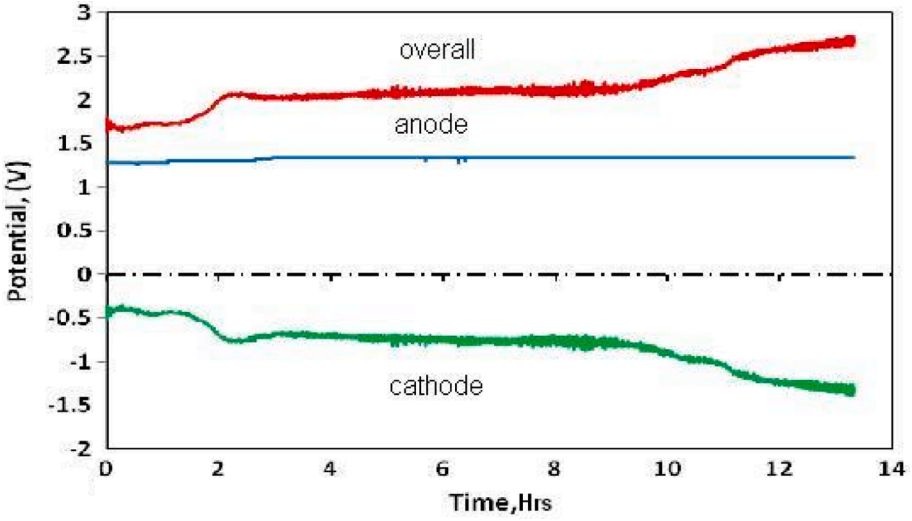

Fig. 9. Chronopotentiogram for the electro-deoxidation of Nb_2O_5 in molten CaO-$CaCl_2$ recorded at 0.2 A.

Appendix A. Supplementary data

Supplementary data to this article can be found online at https://doi.org/10.1016/j.elecom.2023.107435.

References

[1] G.Z. Chen, D.J. Fray, T.W. Farthing, Direct electrochemical reduction of titanium dioxide to titanium in molten calcium chloride, Nature 407 (2000) 361–364.
[2] T. Jiang, X. Xu, G.Z. Chen, Silicon prepared by electro-reduction in molten salts as new energy materials, J. Energy Chem. 47 (2020) 46–61.
[3] Y. Yang, T. Ma, M. Hu, P. Liu, L. Wen, L. Hu, M. Hu, Preparation of CoCrFeNi high-entropy alloy via electro-deoxidation of metal oxides, in: TMS 2020 149th Annual Meeting & Exhibition Supplemental Proceedings. The Minerals, Metals and Materials Series, Springer Cham 2020, pp. 1593-1601.
[4] A.M. Abdelkader, D.J.S. Hyslop, A. Cox, D.J. Fray, Electrochemical synthesis and characterization of a $NdCo_5$ permanent magnet, J. Mater. Chem. 20 (2010) 6039–6049.
[5] A. Mukherjee, R. Kumaresan, K. Joseph, Studies on direct electrochemical de-oxidation of solid ThO_2 in calcium chloride based melts, J. Electrochem. Soc. 168 (2021), 072502.
[6] H. Liu, T. Wu, L. Zhang, X. Wang, H. Li, S. Liu, Q. Zhang, X. Zhang, H. Yu, Germanium nanowires via molten-salt electrolysis for lithium battery anode, ACS Nano 16 (2022) 14402–14411.
[7] A.M. Abdelkader, D.J. Fray, Electrochemical synthesis of hafnium carbide powder in molten chloride bath and its densification, J. Eur. Ceram. Soc. 32 (2012) 4481–4487.
[8] D. Tang, W. Xiao, L. Tian, D. Wang, Electrosynthesis of Ti_2CO_n from TiO_2/C composite in molten $CaCl_2$: effect of electrolysis voltage and duration, J. Electrochem. Soc. 160 (2013) F1192–F1196.
[9] S. Jiao, H. Zhu, Electrolysis of Ti_2CO solid solution prepared by TiC and TiO_2, J. Alloys Compounds 438 (2007) 243–246.
[10] A.M. Abdelkader, D.J. Fray, Synthesis of self-passivated, and carbide-stabilized zirconium nanopowder, J. Nanopart. Res. 15 (2013) 2112.
[11] A.M. Abdelkader, Molten salts electrochemical synthesis of Cr2AlC, J. Eur. Ceram. Soc. 36 (2016) 33–42.
[12] A.M. Abdelkader, Electrochemical synthesis of highly corrugated graphene sheets for high performance supercapacitors, J. Mater. Chem. A 3 (2015) 8519–8525.
[13] A. Meurisse, B. Lomax, Á. Selmeci, M. Conti, R. Lindner, A. Makaya, M.D. Symes, J. Carpenter, Lower temperature electrochemical reduction of lunar regolith simulants in molten salts, Planet. Space Sci. 211 (2022), 105408.
[14] A.M. Abdelkader, K.T. Kilby, A. Cox, D.J. Fray, DC voltammetry of electro-deoxidation of solid oxides, Chem. Rev. 113 (2013) 2863–2886.
[15] W.H. Reinmuth, Distortion of chronopotentiograms from double layer and surface roughness effects, Anal. Chem. 33 (1961) 485–487.
[16] K. Dring, R. Dashwood, D. Inman, Voltammetry of titanium dioxide in molten calcium chloride at 900 degrees C, J. Electrochem. Soc. 152 (2005) E104–E113.
[17] C. Schwandt, D.J. Fray, The electrochemical reduction of chromium sesquioxide in molten calcium chloride under cathodic potential control, Z. Naturforsch. A 62 (2007) 655–670.
[18] A.V. Arakcheeva, V.V. Grinevich, G. Chapuis, V.F. Shamrai, Structure studies of solid solutions of oxygen in electrolytic niobium, Crystallogr. Rep. 47 (2002) 237–244.
[19] U. Stohr, W. Freyland, Intervalence charge transfer and electronic transport in molten salts containing tantalum and niobium complexes of mixed valency, PCCP Phys. Chem. Chem. Phys. 1 (1999) 4383–4387.